

## Aryl butenoic acid derivatives as a new class of histone deacetylase inhibitors: synthesis, in vitro evaluation, and molecular docking studies

Peruze AYHAN EŞİYOK<sup>1</sup>, Özlem SEVEN<sup>1</sup>, Gülüzar EYMUR<sup>1</sup>, Gamze BORA TATAR<sup>2</sup>,  
Didem DAYANGAÇ ERDEN<sup>2</sup>, Kemal YELEKÇİ<sup>3,†</sup>, Hayat YURTER<sup>2,\*,†</sup>,  
Ayhan Sıtkı DEMİR<sup>1,†,\*\*</sup>

<sup>1</sup>Department of Chemistry, Faculty of Arts and Sciences, Middle East Technical University, Ankara, Turkey

<sup>2</sup>Department of Medical Biology, Faculty of Medicine, Hacettepe University, Ankara, Turkey

<sup>3</sup>Department of Computational Biology and Bioinformatics, Faculty of Engineering and Natural Sciences, Kadir Has University, İstanbul, Turkey

Received: 24.05.2013 • Accepted: 08.10.2013 • Published Online: 14.03.2014 • Printed: 11.04.2014

**Abstract:** New aryl butenoic acid derivatives have been synthesized by combining hydroxy- or methoxy-substituted phenyl rings as the capping group, with a double bond in the short linker as well as metal binding groups, enoic ester, and salts bearing either methyl or morpholine. These compounds have been shown to possess promising histone deacetylase inhibition activities via in vitro fluorometric assay and molecular docking studies.

**Key words:** Histone deacetylase inhibition activity, aryl butenoic acid derivatives, molecular docking

### 1. Introduction

Histone acetylase (HAT) and histone deacetylase (HDAC) enzymes act in a competitive manner to determine the histone acetylation levels that ultimately affect the high-order chromatin structure and gene activities at a particular chromosomal region.<sup>1</sup> HDACs reverse the activity of HATs by catalyzing the removal of acetyl groups from lysine residues in the N-terminal tails of histones, leading to chromatin condensation and posttranscriptional gene silencing. To date, 18 HDAC isoforms have been identified and grouped into 3 classes based on homology to yeast HDACs (class I: 1, 2, 3, 8; class II: 4, 5, 6, 7, 9, 10; and class III: SIRT 1–7). HDAC enzymes are gaining more attention, as they deacetylate not only histone but also nonhistone proteins. HDAC inhibitors (HDIs) have been shown to be effective in the treatment of several diseases such as cancer,<sup>2–4</sup> neurodegenerative disorders like proximal spinal muscular atrophy,<sup>5–8</sup> amyotrophic lateral sclerosis, and multiple sclerosis.<sup>9–11</sup>

HDIs can be divided into several structural classes, including short chain fatty acids, hydroxamic acids, epoxyketone-containing cyclic tetrapeptides, epoxyketone-containing cyclic tetrapeptides, and benzamides hybrid molecules. All of these molecules are active exclusively on HDAC class I and class II, by binding to the zinc-containing catalytic domains of the enzymes with different modalities, affinities, and sites.<sup>12</sup> Of these subgroups, hydroxamic acids, including natural inhibitors like trichostatin A (TSA, **1**)<sup>13</sup> and synthesized ones like suberoylanilide hydroxamic acid (SAHA, **2**),<sup>14</sup> are the most potent known HDAC inhibitors, as shown in Figure 1.

\*Correspondence: herdem@hacettepe.edu.tr

† These authors contributed equally to this work.

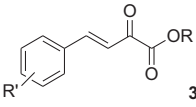
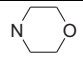
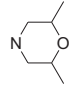
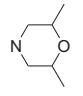
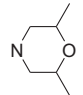
\*\* Deceased (1950–2012).



The best experimental result was obtained with (E)-methyl-4-(3,4-dihydroxyphenyl)-2-oxobut-3-enoate (**3h**) and (E)-4-(4-methoxyphenyl)-1-(2,6-dimethylmorpholino)but-3-ene-1,2-dione (**3j**). P-substituted derivatives have been shown to be better inhibitors compared to m- and o-substituted ones. Salts (**3a**, **3e**, **3f**, and **3g**) were ineffective as inhibitors. Except for the salt derivatives, all the compounds that were tested showed better inhibition compared to NaBA, a well-known HDI (20% experimental inhibition activity). Disubstituted aryl butenoic acid derivatives were also shown to be effective.

When the methyl group was employed in the ester moiety, a higher inhibition occurred, emphasizing this group's zinc-binding ability. This effect has also been visualized from the enhanced activity of dimethyl substituted morpholine compound **3j** compared to the nonsubstituted morpholine compound **3i**.

**Table.** Calculated free energy of binding, inhibition constant and experimental HDAC inhibition activity values of the synthesized compounds.

					
Compound	R'	R	Calculated Free Energy of Binding ( $\Delta G$ , kcal/mol)	Calculated Inhibition Constant ( $K_i$ , $\mu\text{M}$ )	Experimental HDAC Inhibition Activities (%)
3a	4-MeO	$\text{K}^+$	-10.98	0.0089	3
3b	4-MeO	$\text{CH}_3$	-7.08	6.50	53
3c	3-MeO	$\text{CH}_3$	-7.33	4.23	24
3d	2-MeO	$\text{CH}_3$	-7.18	5.48	26
3e	2-OH	$\text{K}^+$	-10.68	0.0142	15
3f	3-OH	$\text{K}^+$	-10.67	0.0151	5
3g	3,4-(OH) <sub>2</sub>	$\text{K}^+$	-10.29	0.0286	4
3h	3,4-(OH) <sub>2</sub>	$\text{CH}_3$	-6.45	18.67	60
3i	4-MeO		-7.34	4.14	51
3j	4-MeO		-7.82	1.86	59
3k	3-MeO		-6.96	7.89	30
3l	2-MeO		-6.96	7.86	33

It should be noted that there were some deviations in the results obtained from the experimental and theoretical data. This might have resulted from the fact that *in silico* studies were carried out with HDAC8 only, while the HeLa nuclear extract contained a variety of HDAC enzymes.

When *in vitro* and *in silico* studies were both taken into consideration, the best inhibition was obtained with (E)-4-(4-methoxyphenyl)-1-(2,6-dimethylmorpholino)but-3-ene-1,2-dione (**3j**), whose interaction

with HDAC8 is shown in Figure 2. The supplementary Figures 1–12 contain 2-D and 3-D pictures of compounds.

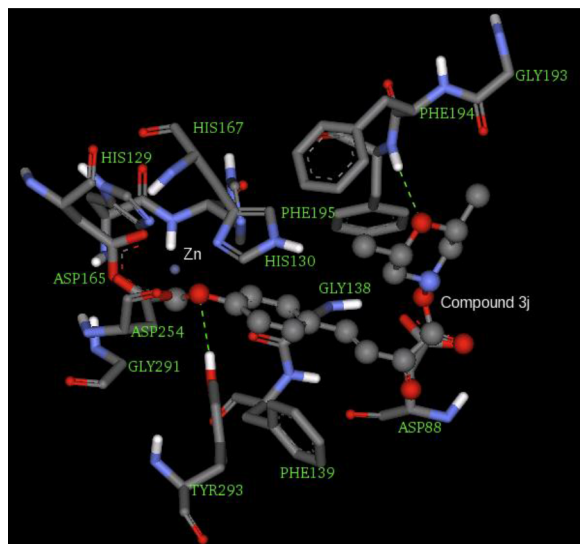


**Figure 2.** Compound **3j** in the active site of the HDAC8 enzyme.

### 3. Experimental

#### 3.1. General procedure for preparation of potassium salts

Pyruvic acid (0.0141 mol) and substituted benzaldehyde (0.0141 mol) were stirred in 1.5 mL of methanol in an ice bath. To this mixture, 5 mL of the alkaline solution of KOH in methanol (1 g in 7.5 mL solvent) was added at 0 °C. Following the removal of the ice bath, the remaining portion of this solution was introduced to the reaction mixture immediately. The resultant mixture was stirred for 1 h at 30 °C and then overnight at 0 °C. A yellow potassium salt was gathered after being filtered and washed with cold methanol and then with ether. The potassium salt was air-dried.<sup>19,20</sup>

#### 3.2. General procedure for preparation of (E)-methyl-4-(aryl)-2-oxobut-3-enoate derivatives<sup>1</sup>

To generate hydrochloric acid, 7 mL acetyl chloride was added to 40 mL of methanol in an ice bath. The potassium salt was added, the reaction mixture was stirred for 30 min, and then the ice bath was removed. After 2 h, the mixture was stirred overnight at 65 °C. The reaction mixture was removed and then 20 mL of water was added and was extracted 2 times with 20 mL of dichloromethane. The organic phase was washed with saturated sodium bicarbonate and then 20 mL of water. The organic phase was dried over anhydrous magnesium sulfate and evaporated. The yellow crystals were obtained via recrystallization from ethanol or methanol.<sup>20,21</sup>

#### 3.3. General procedure of preparation morpholine amide derivatives

In an argon atmosphere, a solution of morpholino derivative (0.454 mmol) in 1.5 mL of toluene was added to a solution of (E)-methyl-4-(aryl)-2-oxobut-3-enoate (0.454 mmol) in 3 mL of toluene, and then 0.2 mL of 2 M triethylaluminum (in heptane) was added. The reaction mixture was stirred at 80 °C for 30 h and cooled to room temperature. Twenty-five milliliters of water was added and extracted 3 times with 25 mL of ethylacetate.

Organic phases were combined and dried over magnesium sulfate, then evaporated. The products were purified with column chromatography (hexane/ethyl acetate, 2:1 or 3:1).

### 3.4. In vitro HDAC inhibition activity screening

HDAC inhibition activity of synthesized compounds was screened by an in vitro fluorometric assay (BioVision) according to the manufacturer's protocol. Briefly, compounds at a 500  $\mu$ M concentration were mixed with HeLa nuclear extract, which contains all HDAC enzyme isoforms. HDAC fluorometric substrate [Boc-Lys(Ac)-AMC], which contains an acetylated lysine side chain, was added to the mixture. Substrate sensitized by deacetylation and the subsequent addition of lysine developer produced fluorophore. Fluorescence was measured with a microplate reader (Molecular Devices Spectramax M2) at excitation 350 nm and emission 440 nm. Screenings were performed in triplicate. Data were analyzed according to decreasing fluorescence signal (arbitrary fluorescence units). The values of treated samples were normalized to nontreated ones, which were set as 100%. NaBA was used as a reference compound, which has 20% HDAC inhibition activity.

### 3.5. AutoDock

AutoDock uses a semiempirical force field based on the AMBER force field.<sup>22–25</sup> It uses a molecular mechanics model for enthalpic contributions, such as vdW and hydrogen bonding, and an empirical model for entropic changes upon binding. Each component is multiplied by empirical weights obtained from the calibration against a set of known binding constants. AutoDock uses a Lamarckian genetic algorithm for the conformational search. For each molecule, 50 independent runs were performed. A total of 300 distinct ligand conformers were initially generated and positioned randomly in the binding pocket. They had randomly assigned torsion angles to rotatable bonds and a randomly assigned overall rotation. A maximum of 100 million energy evaluations was allowed for each docking. A precalculated 3-dimensional energy grid of equally spaced discrete points was generated prior to docking for a rapid energy evaluation, using the program AutoGrid.<sup>4</sup> The grid box, with dimensions of 80 Å  $\times$  80 Å  $\times$  80 Å, was centered near the Zn atom of the active site and covered the entire binding site and its neighboring residues. The distance between 2 grid points was set to 0.375 Å.

#### 3.5.1. Crystal structure of HDAC8

The crystal structures of human histone deacetylase, HDAC8 enzyme (PDB entry code: 1T64, complexed with the inhibitor TSA), was extracted from the Protein Data Bank (<http://www.rcsb.org>). The enzyme structure was cleaned of all water molecules and the irreversible inhibitor of TSA, as well as all noninteracting ions (except zinc) before being used in the docking studies. To relieve the crystal structure tension and to make the protein available to use in the AutoDock<sup>22</sup> docking simulation program, the protein's geometry was first optimized and then submitted to the "Clean Geometry" toolkit of Discovery Studio (Accelrys, Inc.) for a more complete check using a fast Dreiding-like force field. Missing hydrogen atoms were added based on the protonation state of the titratable residues at a pH of 7.4. Ionic strength was set to 0.145 and the dielectric constant was set to 10.

#### 3.5.2. Ligand setups

The 3D structures of ligand molecules were built, optimized at PM3 level, and saved in pdb format with the aid of the molecular modeling program SPARTAN. The AutoDockTools (ADT) graphical user interface programs

were also employed here to generate the docking input files of ligands. ADT helps the user easily set up macromolecules (enzymes) and ligands for docking. It assigns the Gasteiger partial charges to each atom and prepares 2 parameter files, namely a grid parameter file (gpf) and a docking parameter file (dpf). The detail of the procedure is given elsewhere (<http://autodock.scripps.edu>).<sup>26</sup>

#### 4. Conclusions

In this study, new aryl butenoic acid derivatives as HDAC inhibitors have been developed. A privileged structure containing mono or multi methoxy- and hydroxyl-substituted phenyl rings with a carboxylic enoic ester moiety were integrated as a zinc-binding group.

Calculated inhibition values of K salt of compounds **3a**, **3e**, **3f**, and **3g** are in the range of nanomolar concentrations, which is not in agreement with the experimental values. One possible explanation is that, in the calculations, bare carboxylic acid anions were strongly attracted by the zinc ion in the active center. On the other hand, the carboxylate ion may behave differently in the aqueous environment in the active site of the enzyme in in vivo experiments. All the other derivatives showed various degrees of experimental HDAC inhibition activities parallel to computational values. Both morpholine and methyl-substituted enoic esters showed excellent inhibition activity, revealing that both of these groups have zinc-binding capacities. As a conclusion, inhibitor **3j** both experimentally and computationally is the most promising candidate for further HDAC inhibition studies.

#### Acknowledgment

This work was supported by the Scientific and Technological Research Council of Turkey, Research Project No.: 105G014. Patent Application No.: TR 2011 03844 A2.

Supplementary information is available. It includes the experimental details for the syntheses of compounds, and 2-D and 3-D interaction images of the synthesized compounds (**3a–3l**).

#### References

1. Ruijter, A. J. M.; Gennip, A. H.; Caron, H. N.; Kemp, S.; Kuilenburg, A. B. P. *Biochem. J.* **2003**, *370*, 737–749.
2. Santini, V.; Gozzini, A.; Ferrari, G. *Curr. Drug Metab.* **2007**, *8*, 383–394.
3. Bolden, J. E.; Peart, M. J.; Johnstone, R. W. *Nat. Rev. Drug Disc.* **2006**, *5*, 769–784.
4. Liu, T.; Kuljaca, S.; Tee, A.; Marshall, G. M. *Cancer Treat. Rev.* **2006**, *32*, 157–165.
5. Kazantsev, A. G.; Thompson, L. M. *Curr. Drug Metab.* **2007**, *8*, 383–394.
6. Mercuri, E.; Bertini, E.; Messina, S.; Solari, A.; D'Amico, A.; Angelozzi, C.; Batini, R.; Berardinelli, A.; Boffi, P.; Bruno, C. et al. *Neurology* **2007**, *68*, 51–55.
7. Brichta, L.; Holker, I.; Haug, K.; Klockgether, T.; Wirth, B. *Ann. Neurol.* **2006**, *59*, 970–975.
8. Weihl, C. C.; Connolly, A. M.; Pestronk, A. *Neurology* **2006**, *67*, 500–501.
9. Raine, C. S. *J. Neuropathol. Exp. Neurol.* **1994**, *53*, 328–337.
10. McFarland, H. F.; Martin, R. *Nature Immunol.* **2007**, *8*, 913–919.
11. Dheen, S. T.; Kaur, C.; Ling, E. A. *Curr. Med. Chem.* **2007**, *14*, 1189–1197.
12. Drummond, D. C.; Noble, C. O.; Kirpotin, D. B.; Guo, Z.; Scott, G. K.; Benz, C. C. *Ann. Rev. Pharmacol. Toxicol.* **2005**, *45*, 495–528.
13. Yoshida, M.; Kijima, M.; Akita, M.; Beppu, T. *J. Biol. Chem.* **1990**, *265*, 17174–17179.

14. Grant, S.; Easley, C.; Kirkpatrick, P. *Nat. Rev. Drug Discovery* **2007**, *6*, 21–22.
15. Bieliauskas, A. V.; Pflum, M. K. *Chem. Soc. Rev.* **2008**, *37*, 1402–1413.
16. Dayangac-Erden, D.; Bora, G.; Ayhan, P.; Kocaefe, C.; Dalkara, S.; Yelekci, K.; Demir, A. S.; Erdem-Yurter, H. *Chem. Biol. Drug Des.* **2009**, *73*, 355–364.
17. Zeiller, J. J.; Dumas, H.; Guyard-Dangremont, V.; Berard, I.; Contard, F.; Guerrirer, D.; Ferrand, G.; Bonhomme, Y. Patent WO/2005/014521, 2005.
18. Katritzky, A. R.; Feng, D.; Qi, M. *J. Org. Chem.* **1998**, *63*, 1473–1477.
19. Stecher, E. D.; Ryder, H. F. *J. Am. Chem. Soc.* **1952**, *74*, 4392–4395.
20. Audrain, H.; Thorhauge, J.; Hazell, R. G.; Jørgensen, K. A. *J. Org. Chem.* **2000**, *65*, 4487–4497.
21. Wu, Y. C.; Liu, L.; Li, H. J.; Wang, D.; Chen, Y. J. *J. Org. Chem.* **2006**, *71*, 6592–6596.
22. Morris, G. M.; Goodsell, D. S.; Halliday, R. S.; Huey, R.; Hart, W. E.; Belew, R. K.; Olson, A. J. *J. Comput. Chem.* **1998**, *19*, 1639–1662.
23. Weiner, S. J.; Kollman, P. A.; Case, D. A.; Singh, U. C.; Ghio, C.; Alagona, G.; Profeta, S.; Weiner, P. *J. Am. Chem. Soc.* **1984**, *106*, 765–784.
24. Weiner, S. J.; Kollman, P. A.; Nguyen, D. T.; Case, D. A. *J. Comput. Chem.* **1986**, *7*, 230–252.
25. Huey, R.; Morris, G. M.; Olson, A. J.; Goodsell, D. S. *J. Comput. Chem.* **2007**, *28*, 1145–1152.
26. Akdoğan, E. D.; Erman, B.; Yelekçi, K. *Turk. J. Chem.* **2011**, *35*, 523–542.